

Article

## Elastic Properties of $\text{CaSiO}_3$ Perovskite from *ab initio* Molecular Dynamics

Shigeaki Ono <sup>1,2</sup>

<sup>1</sup> Institute for Research on Earth Evolution, Japan Agency for Marine-Earth Science and Technology, 2-15 Natsushima-cho, Yokosuka-shi, Kanagawa 237-0061, Japan; E-Mail: sono@jamstec.go.jp; Tel.: +81-46-867-9631; Fax: +81-46-867-9625

<sup>2</sup> Earthquake Research Institute, University of Tokyo, 1-1-1 Yayoi, Bunkyo-ku, Tokyo 113-0032, Japan

Received: 26 June 2013 / Accepted: 6 October 2013 / Published: 10 October 2013

---

**Abstract:** *Ab initio* molecular dynamics simulations were performed to investigate the elasticity of cubic  $\text{CaSiO}_3$  perovskite at high pressure and temperature. All three independent elastic constants for cubic  $\text{CaSiO}_3$  perovskite,  $C_{11}$ ,  $C_{12}$ , and  $C_{44}$ , were calculated from the computation of stress generated by small strains. The elastic constants were used to estimate the moduli and seismic wave velocities at the high pressure and high temperature characteristic of the Earth's interior. The dependence of temperature for sound wave velocities decreased as the pressure increased. There was little difference between the estimated compressional sound wave velocity ( $V_P$ ) in cubic  $\text{CaSiO}_3$  perovskite and that in the Earth's mantle, determined by seismological data. By contrast, a significant difference between the estimated shear sound wave velocity ( $V_S$ ) and that in the Earth's mantle was confirmed. The elastic properties of cubic  $\text{CaSiO}_3$  perovskite cannot explain the properties of the Earth's lower mantle, indicating that the cubic  $\text{CaSiO}_3$  perovskite phase is a minor mineral in the Earth's lower mantle.

**Keywords:** perovskite; first-principles calculation; seismic wave velocity

**PACS Codes:** 62.20.de; 91.60.Gf

---

### 1. Introduction

Mineral physics constraints on the composition of the Earth's lower mantle rely on knowledge of the equations of state (EOSs) and sound wave velocities in candidate minerals. According to reliable estimates of the composition of the Earth, an  $\text{MgO-FeO-SiO}_2\text{-CaO-Al}_2\text{O}_3$  system could comprise about

99% of the mantle volume [1]. Three minerals have been proposed to be possible hosts of the MgO-FeO-SiO<sub>2</sub>-CaO-Al<sub>2</sub>O<sub>3</sub> system in the Earth's lower mantle. A recent phase equilibrium study using a more representative composition of the mantle shows that Mg, Fe, and Al are mostly accommodated in orthorhombic (Mg,Fe)SiO<sub>3</sub> perovskite and ferropericlaase, (Mg,Fe)O. On the other hand, a number of other experimental studies indicate that the most likely Ca-bearing phase is CaSiO<sub>3</sub> perovskite [2,3]. Thus, the Earth's lower mantle may be composed mainly of aluminous (Mg,Fe)SiO<sub>3</sub> perovskite, CaSiO<sub>3</sub> perovskite, and ferropericlaase. To gain an understanding of the structure and dynamics of the Earth's lower mantle, it is important to investigate the elastic properties of these minerals under the pressure and temperature conditions found in this region. It is easy to investigate the physical properties of orthorhombic (Mg,Fe)SiO<sub>3</sub> perovskite and ferropericlaase, because both minerals can be recovered under ambient conditions. By contrast, CaSiO<sub>3</sub> perovskite is unstable under ambient conditions, and it readily transforms to glass on the release of pressure. Therefore, it is difficult to measure some of its physical properties.

The structure of CaSiO<sub>3</sub> perovskite has tetragonal or orthorhombic symmetry at high pressures and room temperature, e.g., [4,5]. The structure of low-symmetry CaSiO<sub>3</sub> perovskite is still an open question [6–8]. A phase transformation of CaSiO<sub>3</sub> perovskite from this low symmetry into cubic symmetry with an increase in temperature was found in a previous study [5], indicating that the cubic structure of CaSiO<sub>3</sub> perovskite is stable under the conditions of the Earth's lower mantle, and that its physical properties are important for understanding the dynamics and evolution of the Earth's interior. The elastic properties of cubic CaSiO<sub>3</sub> perovskite were calculated at 0 K [9,10] and high temperatures [8]. These data relating to the elastic properties of cubic CaSiO<sub>3</sub> perovskite are insufficient to discuss the composition of the Earth's lower mantle, because an internally consistent data set describing the density- $V_P$ - $V_S$  relationship in cubic CaSiO<sub>3</sub> perovskite is needed in order to compare the density- $V_P$ - $V_S$  relationship of a preliminary reference earth model (PREM) [11] with that estimated based on cubic CaSiO<sub>3</sub> perovskite. Therefore, it is necessary to reevaluate the density- $V_P$ - $V_S$  relationship using *ab initio* calculations.

We employed the *ab initio* molecular dynamics (AIMD) method using density functional theory (DFT) to determine the density values and sound wave velocities for cubic CaSiO<sub>3</sub> perovskite at pressures typical of the Earth's lower mantle. We also used the experimental data to correct the calculated values of the density and the sound wave velocities for cubic CaSiO<sub>3</sub> perovskite.

## 2. Method

We performed the AIMD calculations based on DFT using the VASP code [12]. The interactions between the electrons and the ionic cores were described using the projector augmented wave (PAW) method [13] with generalized gradient approximations, known as PBE [14]. The advantage of this code is that the *ab initio* energy of the system can be combined with the molecular dynamics method to simulate the properties of cubic CaSiO<sub>3</sub> perovskite at high pressure and high temperature simultaneously. The PAW potentials of Ca, Si, and O had core radii of 2.3, 1.5, and 1.1 a.u., respectively. Single particle orbitals were expanded in plane waves, with a plane-wave cut-off of 900 eV. The calculations were performed on the basis of a self-consistency convergence on the total energy of 10<sup>-4</sup> eV per simulation cell. We used a 135-atom supercell, with  $\Gamma$ -point Brillouin zone sampling and a

time step of 1 fs at a constant volume. The simulations were run in the constant  $NVT$  ensemble with a Nosé thermostat [15] for at least 5 ps after equilibration. The computation time required to reach equilibrium varied between configurations, and depended on the starting atomic position, velocity, temperature, and pressure. In previous studies, we have confirmed that useful data for the elastic properties of solids in high pressure and temperature conditions can be acquired using the previous AIMD calculations, e.g., [16,17]. In this study, AIMD calculations were performed under 27 selected pressure and temperature conditions up to 175 GPa and 4000 K. A comprehensive description of our method as applied to the modeling of condensed matter has been described previously [18].

The elastic constants can be determined from the computation of the stress generated by small strains [19]. For a cubic crystal, the three elastic moduli,  $C_{11}$ ,  $C_{12}$ , and  $C_{44}$ , fully describe its elastic behavior. The values of  $C_{11}$  and  $C_{12}$  can be determined from the bulk modulus  $K$  and shear constant  $C_S$ :

$$K = (C_{11} + 2C_{12})/3 \quad (1)$$

$$C_S = (C_{11} - C_{12})/2 \quad (2)$$

The following tetragonal strains were applied to obtain  $C_S$ :

$$\varepsilon = \begin{pmatrix} e & 0 & 0 \\ 0 & e & 0 \\ 0 & 0 & (1+e)^{-2} - 1 \end{pmatrix} \quad (3)$$

where  $e$  is the strain magnitude. The change in the free energy of the strained structure,  $\Delta E(e)$ , is related to  $e$  as follows:

$$\Delta E(e) = 3V(C_{11} - C_{12})e^2 + O(e^3) \quad (4)$$

where  $V$  is the volume of the cell.  $C_{44}$  was calculated by applying the volume-conserving orthorhombic strain:

$$\varepsilon = \begin{pmatrix} 0 & e & 0 \\ e & 0 & 0 \\ 0 & 0 & e^2/(1-e^2) \end{pmatrix} \quad (5)$$

The energy associated with this strain is:

$$\Delta E(e) = 2C_{44}Ve^2 + O(e^4) \quad (6)$$

According to the calculations for unstrained and strained structures, the elasticity of cubic  $\text{CaSiO}_3$  perovskite at high pressure and high temperature can be determined.

### 3. Results

The EOS of cubic  $\text{CaSiO}_3$  perovskite has been investigated in a previous experimental study [20]. Recent theoretical studies have investigated the physical properties of materials under high pressure and high temperature using first-principles calculations. We noticed that the scatter of the EOS determined by experimental study was smaller than that obtained from first-principles calculations [18], indicating that the EOS determined in experiments was more accurate than that determined from first-principles calculations. By contrast, the AIMD calculations present significant advantages for

investigating the elastic properties of materials under high temperatures and high temperatures. Therefore, we used the experimental data to determine the EOS for cubic CaSiO<sub>3</sub> perovskite. The pressures estimated by the AIMD calculations were corrected based on the EOS determined by the experimental data. The combination of first-principles molecular dynamics calculations and high pressure experimental data led us to determine reliable physical properties over a wide range of pressures and temperatures. The EOS for a solid can be described in a general form as a functional relationship between pressure, volume, and temperature:

$$P_{Total}(V, T) = P_{st}(V, 300) + P_{th}(V, T) \quad (7)$$

A fit of the volume-pressure data yielded volume and bulk modulus values of  $V_0 = 45.58 \text{ \AA}^3$ ,  $K_{T0} = 236 \text{ GPa}$  and  $K'_{T0} = 3.9$  [20] for a third-order Birch-Murnaghan EOS [21]:

$$P_{st} = \frac{3}{2} K_{T0} \left[ \left( \frac{V_0}{V} \right)^{\frac{7}{3}} - \left( \frac{V_0}{V} \right)^{\frac{5}{3}} \right] \left\{ 1 - \frac{3}{4} (4 - K'_{T0}) \left[ \left( \frac{V_0}{V} \right)^{\frac{2}{3}} - 1 \right] \right\} \quad (8)$$

where  $V_0$  and  $K_{T0}$ , and  $K'_{T0}$  are the volume, isothermal bulk modulus, and first pressure derivative of the isothermal bulk modulus, respectively. The thermal pressure,  $P_{th}$ , of the thermal pressure EOS can be written as follows:

$$P_{th} = \left[ \alpha K_T(V_0, T) + \left( \frac{\partial K_T}{\partial T} \right)_V \ln \left( \frac{V_0}{V} \right) \right] (T - T_0) \quad (9)$$

A least squares fit of the high temperature data from the AIMD calculations yields  $\alpha K_T(V_0, T) = 0.0083$  and  $(\partial K_T / \partial T)_V = -0.0031$ . The value of  $P_{th}$  of cubic CaSiO<sub>3</sub> perovskite was not sensitive to changes in volume at the pressures investigated in this study, because the values of  $(\partial K_T / \partial T)_V$  were very small. The fitting parameters of the third-order Birch-Murnaghan EOS combined with the thermal pressure EOS were  $V_0$ ,  $K_{T0}$ ,  $K'_{T0}$ ,  $\alpha K_T(V_0, T)$ , and  $(\partial K_T / \partial T)_V$ . The results of the fit of our  $P$ - $V$ - $T$  data to the thermal pressure equation of state are summarized in Table 1.

**Table 1.** The thermoelastic parameters of cubic CaSiO<sub>3</sub> perovskite. The third-order Birch–Murnaghan EOS was used to calculate the parameters of cubic CaSiO<sub>3</sub> perovskite. Key:  $K_{T0}$ , isothermal bulk modulus at 0 GPa and 300 K;  $K'_{T0}$ , first pressure derivation of the bulk modulus;  $V_0$ , volume at 0 GPa and 300 K. The terms  $\alpha K_T(V_0, T)$  and  $(\partial K_T / \partial T)_V$  are parameters of the thermal pressure.

Parameter	Value
$V_0$ ( $\text{\AA}^3$ )	45.58 <sup>a</sup>
$K_{T0}$ (GPa)	236 <sup>a</sup>
$K'_{T0}$	3.9 <sup>a</sup>
$\alpha K_T(V_0, T)$ (GPa/K)	0.0083(3)
$(\partial K_T / \partial T)_V$ (GPa/K)	-0.0031(31)

<sup>a</sup> The parameters are from Shim *et al.* [20].

We determined the elastic constant by computing the stress generated by small deformations of the equilibrium cell. Figure 1 shows three elastic constants of cubic CaSiO<sub>3</sub> perovskite ( $C_{11}$ ,  $C_{12}$  and  $C_{44}$ ) at

2000 K as a function of pressure up to 160 GPa. The bulk modulus of an isotropic aggregate cubic crystal is well defined, whereas the shear modulus can be constrained by the Voigt-Reuss-Hill scheme [22]:

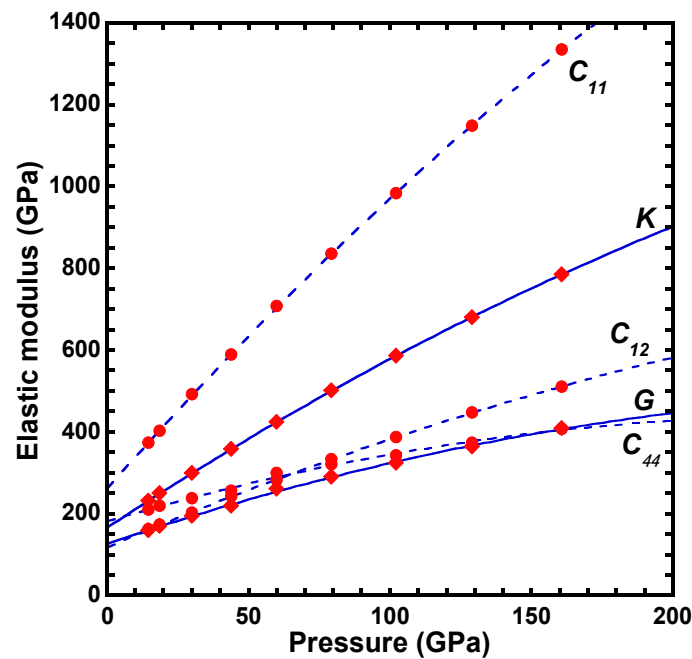
$$G^V = \frac{1}{5}(2C_s + 3C_{44}) \tag{10}$$

$$G^R = \left[ \frac{1}{5} \left( \frac{2}{C_s} + \frac{3}{C_{44}} \right) \right]^{-1} \tag{11}$$

$$G^H = \frac{1}{2}(G^V + G^R) \tag{12}$$

We also show the bulk modulus  $K$  and Hill’s average  $G$  at 2000 K as a function of pressure in Figure 1. Karki and Crain [9] calculated elastic constants and moduli of cubic  $\text{CaSiO}_3$  perovskite at 0 K up to 140 GPa. Our results for elastic parameters calculated at 2000 K were in general agreement with those at 0 K reported by previous studies.

**Figure 1.** Pressure dependence of three elastic constants,  $C_{11}$ ,  $C_{12}$ , and  $C_{44}$ , and the isotropic bulk ( $K$ ) and shear ( $G$ ) moduli of cubic  $\text{CaSiO}_3$  perovskite at 2000 K. The solid circles and diamonds represent the elastic constants and the elastic moduli, respectively. The solid and dashed lines are the fits of each parameter.



The three isotropically averaged aggregate sound velocities could be derived from the bulk modulus  $K$  and shear modulus  $G$ :

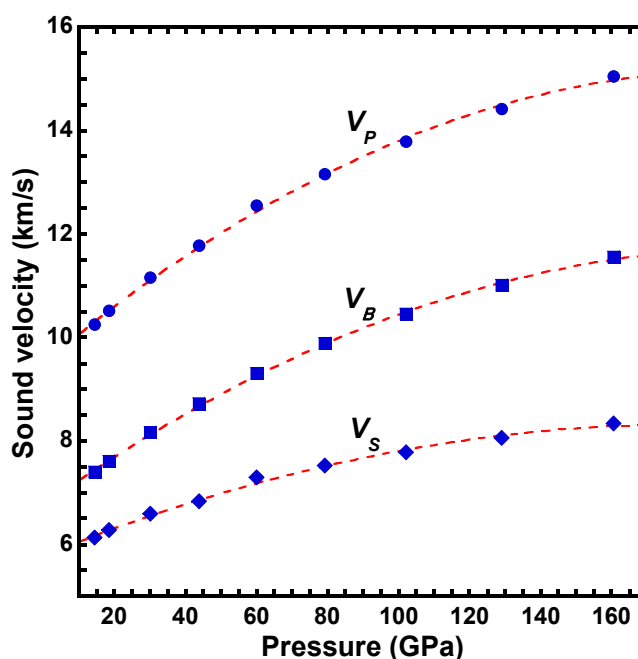
$$V_p = \left[ \left( K + \frac{4}{3}G \right) / \rho \right]^{\frac{1}{2}} \tag{13}$$

$$V_b = \left( \frac{K}{\rho} \right)^{\frac{1}{2}} \tag{14}$$

$$V_S = \left( \frac{G}{\rho} \right)^{\frac{1}{2}} \quad (15)$$

where  $V_P$ ,  $V_B$ , and  $V_S$  are the compressional, bulk, and shear sound wave velocities, respectively, and  $\rho$  is the density. The three sound wave velocities,  $V_P$ ,  $V_B$ , and  $V_S$ , increased with increasing pressure at 2000 K in Figure 2. Our results for sound wave velocities were in good agreement with those reported by Li *et al.* [8].

**Figure 2.** Sound wave velocities in cubic CaSiO<sub>3</sub> perovskite at 2000 K calculated from the elastic constants. The solid circles, squares, and diamonds represent the compressional, bulk, and shear velocities, respectively.



The effect of temperature on the sound wave velocities was investigated at high temperatures corresponding to conditions in the Earth's mantle. In Figure 3, the results of the AIMD simulations at high temperatures of  $2000 \leq T(\text{K}) \leq 4000$  showed that sound wave velocities decreased with increasing temperature. However, there were only small dependencies on temperature. As the pressure increased, these dependencies on temperature became small. The sound wave velocities were fitted to the following equation as functions of temperature and pressure:

$$v = a + (b + cP)T + d \ln(P) \quad (16)$$

where  $a$ ,  $b$ ,  $c$  and  $d$  are fitted parameters, and  $T$  and  $P$  are given in K and GPa, respectively. The results of the fitted parameters are summarized in Table 2.

**Figure 3.** Sound wave velocities in cubic CaSiO<sub>3</sub> perovskite at high temperatures. The diamonds represent the compressional and shear wave velocities calculated by the AIMD simulations. The dashed lines represent the fitted velocities for 2000, 3000, and 4000 K.

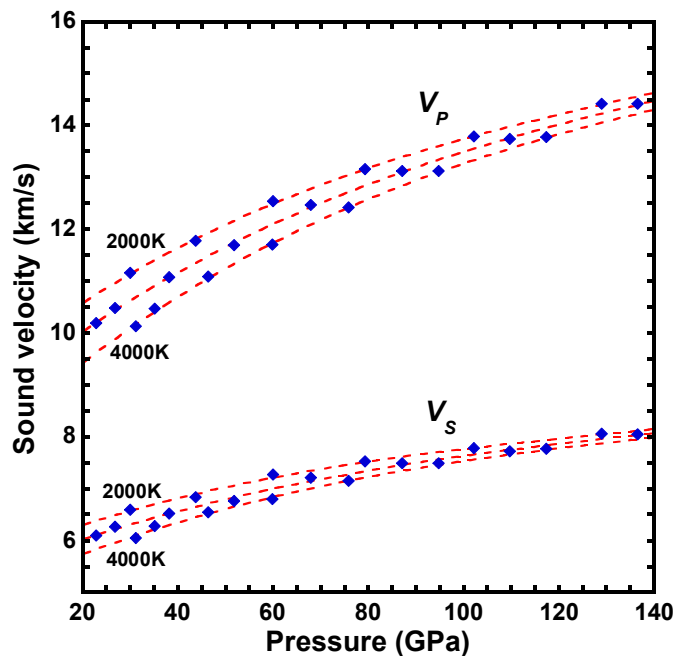


**Table 2.** Parameters of the compressional and shear sound velocities. The parameters are given by  $v = a + (b + cP)T + d \ln(P)$ , where  $T$  and  $P$  are the temperature (K) and the pressure (GPa), respectively. The conditions for applying these parameters to Equation (16) are  $15 \text{ GPa} < P < 140 \text{ GPa}$  and  $1500 \text{ K} < T < 4500 \text{ K}$ .

	$a$	$b$	$c$	$d$
$V_P$	7.12(0.27)	$-6.96(0.33) \times 10^{-4}$	$4.07(0.30) \times 10^{-7}$	1.56(0.06)
$V_S$	4.65(0.15)	$-3.20(0.02) \times 10^{-4}$	$1.75(0.17) \times 10^{-6}$	0.74(0.04)

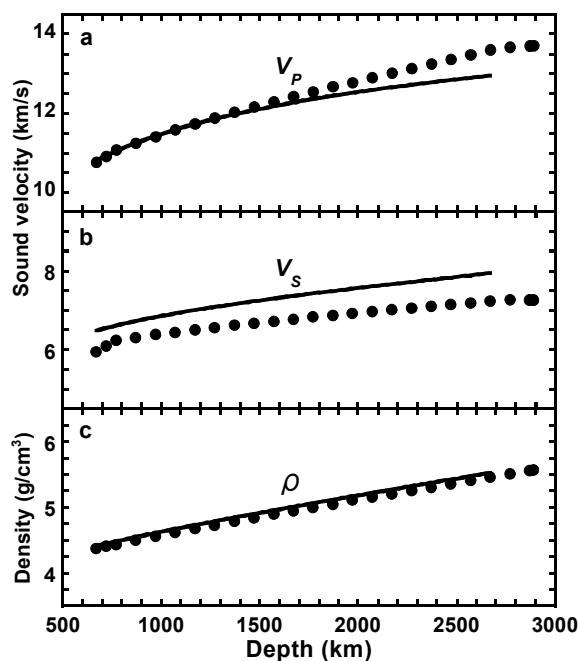
#### 4. Discussion

It is important to assess the uncertainties of the *ab initio* calculations to understand the implications of the calculated results. In general, different types of approximation have led to different values in previous *ab initio* studies, e.g., [18]. The difference between Local Density Approximation (LDA) and Generalized Gradient Approximation (GGA) leads to a change in cell volume of a few percent. This uncertainty is non-negligible in the context of discussing the behavior of the Earth's mantle. Although GGA was used in the present study, we corrected the calculated values according to the experimental EOS to minimize the uncertainties related to approximations used in *ab initio* simulations. Therefore, our discussion of the comparison between estimated elastic properties and PREM values is more reliable than those of previous studies.

It is believed that the lower mantle contains three minerals; (Fe,Al)-bearing Mg-perovskite, ferropericlasite, and Ca-perovskite [2,3]. We calculated the density, and the compressional and shear sound wave velocities for cubic CaSiO<sub>3</sub> perovskite in order to compare them with the values from the PREM [11]. The values for cubic CaSiO<sub>3</sub> perovskite were calculated using the EOS defined in Table 1

and Equation (16) defined in Table 2. The estimated values for cubic  $\text{CaSiO}_3$  perovskite and the PREM are compared in Figure 4. The adiabatic temperature profile (geotherm) was used as the temperature profile in the Earth's lower mantle [3]. The calculated density of cubic  $\text{CaSiO}_3$  perovskite was in good agreement with that estimated by seismological data (PREM). Li *et al.* [8] estimated the density of cubic  $\text{CaSiO}_3$  perovskite, and the estimated density was higher than that in the PREM data. Although our AIMD method was similar to that used by Li *et al.* [8], the discrepancy between this and the previous study was confirmed. As the pressure was corrected to estimate density accurately in this study, the difference between our estimated density of cubic  $\text{CaSiO}_3$  perovskite and that from the PREM data should be small. For the compressional sound wave velocity, the discrepancy between the calculated values for cubic  $\text{CaSiO}_3$  perovskite and the observed data was small. The difference increased as the depth increased. By contrast, the shear sound wave velocity in cubic  $\text{CaSiO}_3$  perovskite was much higher than that from the PREM data. If cubic  $\text{CaSiO}_3$  perovskite is a major mineral in the Earth's lower mantle, the sound wave velocity profiles cannot be explained. Therefore, our study implies that cubic  $\text{CaSiO}_3$  perovskite is a minor mineral in the Earth's lower mantle. In a previous study, that the shear sound wave velocity in orthorhombic  $(\text{Mg,Fe})\text{SiO}_3$  perovskite was reported to be lower than that in cubic  $\text{CaSiO}_3$  perovskite at 0 K [23]. As the shear sound wave velocity in ferropericlase,  $(\text{Mg,Fe})\text{O}$ , is much lower than that of orthorhombic  $(\text{Mg,Fe})\text{SiO}_3$  perovskite, sound wave velocities in orthorhombic  $(\text{Mg,Fe})\text{SiO}_3$  perovskite at higher temperatures are therefore in general agreement with those from PREM, indicating that orthorhombic  $(\text{Mg,Fe})\text{SiO}_3$  perovskite might be a major mineral in the Earth's lower mantle.

**Figure 4.** Density and sound wave velocities for cubic  $\text{CaSiO}_3$  perovskite compared with PREM data. The solid circles represent the values from PREM [11]. The solid lines represent the calculated values under the conditions of the Earth's lower mantle. The values for cubic  $\text{CaSiO}_3$  perovskite were calculated using the equations defined in Tables 1 and 2 and the adiabatic temperature profile (geotherm) in the Earth's interior [3]; a: compressional sound velocity; b: shear sound velocity; c: density.



In general, a certain quantity of most elements dissolves in three minerals, namely (Fe,Al)-bearing Mg-perovskite, ferropervicase, and Ca-perovskite, and the partition coefficients of minor elements between the three minerals change with temperature and pressure. In this study, the physical properties of a pure cubic CaSiO<sub>3</sub> perovskite host were calculated, because the complicated chemical composition would need a very large simulation time, and it would have been difficult to perform a reliable AIMD study. The effects of the minor elements on the density and the sound wave velocities therefore require further investigation.

## 5. Conclusions

We have predicted from the first-principles theory the sound velocities of cubic CaSiO<sub>3</sub> perovskite at high pressures and temperatures corresponding to the Earth's lower mantle. Comparison of the elastic properties of cubic CaSiO<sub>3</sub> perovskite with the lower mantle properties estimated from the seismic observations supports the prevailing hypothesis that the lower mantle consists primarily of (Mg,Fe)SiO<sub>3</sub> perovskite.

## Acknowledgments

This work made use of the super computer system of JAMSTEC and of the computer systems of the Earthquake Information Center of the Earthquake Research Institute. This work was supported by Grant-in-Aid for Scientific Research from JSPS and the Earthquake Research Institute cooperative research program, Japan.

## Conflicts of Interest

The author declares no conflict of interest.

## References

1. Anderson, D.L. Composition of the Earth. *Science* **1989**, *243*, 367–370.
2. Irifune, T.; Ringwood, A.E. Phase Transitions in Primitive MORB and Pyrolite Compositions to 25 GPa and Some Geophysical Implications. In *High-Pressure Research in Mineral Physics*; Manghnani, M.H., Syono, Y., Eds.; Terra Scientific Publishing Company, Tokyo/American Geophysical Union: Washington, DC, USA, 1987; pp. 231–242.
3. Ono, S. Experimental constraints on the temperature profile in the lower mantle. *Phys. Earth Planet. Inter.* **2008**, *170*, 267–273.
4. Shim, S.H.; Jeanloz, R.; Duffy, T.S. Tetragonal structure of CaSiO<sub>3</sub> perovskite above 20 GPa. *Geophys. Res. Lett.* **2002**, *29*, doi:10.1029/2002GL016148.
5. Ono, S.; Ohishi, Y.; Mibe, K. Phase transition of Ca-perovskite and stability of Al-bearing Mg-perovskite in the lower mantle. *Am. Mineral.* **2004**, *89*, 1480–1485.
6. Caracas, R.; Wentzcovitch, R.; Price, G.D.; Brodholt, J. CaSiO<sub>3</sub> perovskite at lower mantle pressures. *Geophys. Res. Lett.* **2005**, *32*, L06306.
7. Adams, D.J.; Oganov, A.R. *Ab initio* molecular dynamics study CaSiO<sub>3</sub> perovskite at *P-T* conditions of Earth's lower mantle. *Phys. Rev. B* **2006**, *73*, 184106.

8. Li, L.; Weidner, D.J.; Brodholt, J.; Alfè, D.; Price, G.D.; Caracas, R.; Wentzcovitch, R. Phase stability of CaSiO<sub>3</sub> perovskite at high pressure and temperature: Insights from *ab initio* molecular dynamics. *Phys. Earth Planet. Inter.* **2006**, *155*, 260–268.
9. Karki, B.B.; Crain, J. First-principles determination of elastic properties of CaSiO<sub>3</sub> perovskite at lower mantle pressures. *Geophys. Res. Lett.* **1998**, *25*, 2741–2744.
10. Stixrude, L.; Lithgow-Bertelloni, C.; Kiefer, B.; Fumagalli, P. Phase stability and shear softening in CaSiO<sub>3</sub> perovskite at high pressure. *Phys. Rev. B* **2007**, *75*, 024108.
11. Dziewonski, A.M.; Anderson, D.L. Preliminary reference earth model. *Phys. Earth Planet. Inter.* **1981**, *25*, 297–356.
12. Kresse, G.; Furthmüller, J. Efficient iterative schemes for *ab initio* total-energy calculations using a plane-wave basis set. *Phys. Rev. B* **1996**, *54*, 11169–11186.
13. Blöchl, P.E. Projector augmented-wave method. *Phys. Rev. B* **1994**, *50*, 17953–17979.
14. Perdew, J.P.; Burke, K.; Ernzerhof, M. Generalized gradient approximation made simple. *Phys. Rev. Lett.* **1996**, *77*, 3865–3868.
15. Nosé, S. A molecular dynamics method for simulations in the canonical ensemble. *Mol. Phys.* **1984**, *52*, 255–268.
16. Ono, S.; Brodholt, J.P.; Alfè, D.; Alfredsson, M.; Price, G.D. *Ab initio* molecular dynamics simulations for thermal equation of state of B2-type NaCl. *J. Appl. Phys.* **2008**, *86*, 5801–5808.
17. Ono, S. First-principles molecular dynamics calculations of the equation of state for tantalum. *Int. J. Mol. Sci.* **2009**, *10*, 4342–4351.
18. Ono, S. Synergy Between First-Principles Computation and Experiment in Study of Earth Science. In *Some Applications of Quantum Mechanics*; Pahlavani, M.R., Ed.; InTech: Vienna, Austria, 2012; pp. 91–108.
19. Mehl, M.J.; Osburn, J.E.; Papaconstantopoulos, D.A.; Klein, B.M. Structural properties of ordered high-melting-temperature intermetallic alloys from first-principles total-energy calculations. *Phys. Rev. B* **1990**, *41*, 10311–10323.
20. Shim, S.H.; Duffy, T.S. The stability and P-V-T equation of state of CaSiO<sub>3</sub> perovskite in the Earth's lower mantle. *J. Geophys. Res.* **2000**, *105*, 25955–25968.
21. Poirier, J.P. *Introduction to the Physics of the Earth's Interior*; Cambridge University Press: Cambridge, UK, 2000.
22. Anderson, O.L. *Equations of State of Solids for Geophysics and Ceramic Science*; Oxford University Press: New York, NY, USA, 1995.
23. Karki, B.B.; Stixrude, L. Seismic velocities of major silicate and oxide phases of the lower mantle. *J. Geophys. Res.* **1999**, *104*, 13025–13033.